Revisiting Random Weight Perturbation for Efficiently Improving Generalization

Anonymous authors
Paper under double-blind review

Abstract

Improving the generalization ability of modern deep neural networks (DNNs) is a fundamental challenge in machine learning. Two branches of methods have been proposed to seek flat minima and improve generalization: one led by sharpness-aware minimization (SAM) minimizes the worst-case neighborhood loss through adversarial weight perturbation (AWP), and the other minimizes the expected Bayes objective with random weight perturbation (RWP). While RWP offers advantages in computation and is closely linked to AWP on mathematical basis, its empirical performance has consistently lagged behind that of AWP. In this paper, we revisit the use of RWP for improving generalization and propose improvements from two perspectives: convergence and perturbation generation. Through extensive experimental evaluations, we demonstrate that our enhanced RWP methods achieve greater efficiency in enhancing generalization, particularly in large-scale problems, while also offering comparable or even superior performance to SAM through AWP. The code will be released.

1 Introduction

Modern deep neural networks (DNNs) are commonly characterized by their over-parameterization, boasting millions or even billions of parameters. This extensive model capacity empowers DNNs to explore a vast hypothesis space and achieve state-of-the-art performance across various domains (Tan & Le, 2019; Kolesnikov et al., 2020; Liu et al., 2021; Radford et al., 2021). However, this abundance of parameters relative to the number of training samples makes DNNs prone to memorizing the training data, leading to overfitting issues. Consequently, it becomes crucial to develop effective training algorithms that facilitate generalization beyond the training set (Neyshabur et al., 2017).

Numerous studies have been dedicated to improving the generalization ability of DNNs (Szegedy et al., 2016; Izmailov et al., 2018; Zhang et al., 2018; 2019; Foret et al., 2020). Building upon the notion that flat minima are better suited to adapt to potential distribution shifts between training and test data, leading to improved generalization (Hochreiter & Schmidhuber, 1997; Dinh et al., 2017; Li et al., 2018), two prominent branches of methods have emerged to identify and exploit such flat minima for effective generalization improvement. The first branch formulates the optimization objective as a min-max problem, aiming to minimize the training loss under the worst-case adversarial weight perturbation (AWP). This approach, also known as sharpness-aware minimization (SAM) (Foret et al., 2020), seeks to find flat minima that reside in neighborhoods characterized by consistently low loss values. The second branch, exemplified by LPF-SGD (Bisla et al., 2022), aims to recover flat minima by minimizing the expected training loss through random weight perturbation (RWP). Notably, these two approaches share similarities in their formulations and can be mathematically connected (Möllenhoff & Khan, 2023).

Despite achieving state-of-the-art generalization performance, AWP, represented by SAM (Foret et al., 2020), suffers from a significant drawback in terms of computation and training time. This is due to the involvement of two gradient steps, which doubles the computational requirements. Consequently, applying AWP to large-scale problems becomes a prohibitive challenge. On the other hand, RWP offers a more computationally efficient alternative, requiring only negligible additional computational overhead compared to regular training. However, it is commonly believed that RWP exhibits inferior empirical performance when compared to AWP

(Zheng et al., 2021; Liu et al., 2022b). This discrepancy can be attributed to the fact that RWP perturbs the model with less intensity than AWP, which benefits from leveraging precise gradient information.

In this paper, we revisit the use of RWP for improving generalization and aim to bridge the performance gap between these two types of perturbations. We begin by demonstrating that RWP necessitates orders of magnitude larger perturbations compared to AWP to achieve similar perturbation strength, which can lead to convergence issues. To address this challenge, we propose a simple approach called mixed-RWP, or m-RWP, which incorporates the gradient of the original loss objective to improve convergence and guide the network towards better minima. Notably, although both SAM and m-RWP require two gradient steps per iteration, m-RWP is more efficient in improving generalization, which lies two aspects: 1) in m-RWP, these two steps are separable and can be efficiently computed *in parallel*, enabling the same training speed as regular SGD. In contrast, the two gradient steps in SAM are successive, resulting in a doubling of the training time. 2) the two separable gradient steps in m-RWP allow simultaneous use *two different batches* of data, further accelerating the convergence, especially on large-scale datasets. In contrast, SAM does not allow for the use of two different batches and may even negatively impact generalization performance. The improved convergence of m-RWP also allows for a larger perturbation radius to confer better generalization performance. Furthermore, we enhance the generation of random weight perturbation by incorporating historical gradient information as guidance. This improvement enables more stable and adaptive weight perturbation generation, leading to enhanced performance. As a result, we significantly boost the generalization performance of RWP and introduce two improved RWP approaches: 1) ARWP which achieves competitive performance to AWP but requires only half of the computation and 2) m-ARWP which achieves comparable or even superior performance while benefiting from parallel computing of the two gradient steps.

In summary, we make the following contributions:

- We analyze the convergence properties of SGD with RWP in non-convex settings and identify potential convergence issues due to the larger perturbation magnitude required by RWP compared to AWP. We then suggest a simple method to enhance the convergence of RWP.
- We propose an improvement to the generation of random weight perturbation by utilizing historical gradient information. This enhancement enables more stable and adaptive generation of weight perturbations, leading to improved performance.
- We present a comprehensive empirical study showing that our improved RWP approaches can achieve more efficient generalization improvements compared to AWP, especially on large-scale problems.

2 Related Work

Flat Minima and Generalization. The connection between the flatness of local minima and generalization has been extensively studied (Dinh et al., 2017; Keskar et al., 2017; Izmailov et al., 2018; Li et al., 2018; Jiang* et al., 2020). Hochreiter *et al.* (Hochreiter & Schmidhuber, 1994; 1997) are among the first to reveal the connection between flat minima and the generalization of a model. Keskar *et al.* (Keskar et al., 2017) observe that the performance degradation of large batch training is caused by converging to sharp minima. More recently, Jiang *et al.* (Jiang* et al., 2020) present a large-scale study of generalization in DNNs and demonstrate a strong connection between the sharpness and generalization error under various settings and hyper-parameters. Keskar *et al.* (Keskar et al., 2017) and Dinh *et al.* (Dinh et al., 2017) state that the flatness can be characterized by Hessian's eigenvalues and provide computationally feasible method to measure it.

Sharpness-aware Minimization (SAM). SAM (Foret et al., 2020) is a recently proposed training scheme that seeks flat minima by formulating a min-max problem and utilizing adversarial weight perturbation (AWP) to encourage parameters to sit in neighborhoods with uniformly low loss. It has shown power to achieve state-of-the-art performance. Later, a line of works improves the SAM's performance from the perspective of the neighborhood's geometric measure (Kwon et al., 2021; Kim et al., 2022; Liu et al., 2022b) or surrogate loss function (Zhuang et al., 2022). Several methods have been developed to improve training efficiency (Du et al., 2022a;b; Liu et al., 2022a; Mi et al., 2022; Zhao et al., 2022b;b; Jiang et al., 2023).

Random Weight Perturbation (RWP). RWP is widely used in deep learning. Multiple weight noise injection methods have been shown to effectively escape spurious local optimum (Zhou et al., 2019) and saddle points (Jin et al., 2021). Upon generalization, Zhang *et al.* (Zheng et al., 2021) discuss that RWP is much less effective for generalization improvement than AWP. Wen *et al.*. (Wen et al., 2018) propose SmoothOut framework to smooth out the sharp minima. Wang & Mao (2021) propose Gaussian model perturbation (GMP) as a regularization scheme for SGD training, but it remains inefficient due to the need of multiple computation budgets for noise sampling. Bisla *et al.* (Bisla et al., 2022) connect the smoothness of the loss objective to generalization and adopt filter-wise random Gaussian perturbation generation to improve the performance. However, the performance of RWP still lags behind that of AWP (Bisla et al., 2022; Liu et al., 2022b). Notably, recent Möllenhoff *et al.* (Möllenhoff & Khan, 2023) mathematically connect the expected Bayes loss under RWP with the min-max loss in SAM and suggest that RWP can be viewed as a 'softer' version of AWP. We significantly lift the performance of RWP from the convergence perspective and fill the performance gap to that of AWP.

3 Preliminary

Let $f(\boldsymbol{x}; \boldsymbol{w})$ be the neural network function with trainable parameters $\boldsymbol{w} \in \mathbb{R}^d$, where d is the number of parameters. The loss function over a pair of data point $(\boldsymbol{x}_i, \boldsymbol{y}_i)$ is denoted as $L(f(\boldsymbol{x}_i; \boldsymbol{w}), \boldsymbol{y}_i)$ (shorted for $L_i(\boldsymbol{w})$). Given the datasets $\mathcal{S} = \{(\boldsymbol{x}_i, \boldsymbol{y}_i)\}_{i=1}^n$ drawn from data distribution $\mathcal{D}$ with i.i.d. condition, the empirical loss can be defined as $L(\boldsymbol{w}) = \frac{1}{n}\sum_{i=1}^n L_i(\boldsymbol{w})$.

Two branches of methods are proposed to pursue flat minima and better generalization ability. The first, known as sharpness-aware minimization (Foret et al., 2020), tries to minimize the worst-case loss in a neighborhood (defined by a norm ball) to bias training trajectories towards flat minima, i.e.,

$$L^{\text{SAM}}(\boldsymbol{w}) = \max_{\|\boldsymbol{\epsilon}_s\|_2 \leq \rho} L(\boldsymbol{w} + \boldsymbol{\epsilon}_s), \tag{1}$$

where ρ is the radius that controls the neighborhood size. Instead of posing the strict 'max-loss' over the neighborhood, the second, represented by LPF-SGD (Bisla et al., 2022), adopts 'expected-loss' and minimizes the posterior (typically an isotropic Gaussian distribution) of the following Bayes objective (Möllenhoff & Khan, 2023):

$$L^{\text{Bayes}}(\boldsymbol{w}) = \mathbb{E}_{\boldsymbol{\epsilon}_r \sim \mathcal{N}(\mathbf{0}, \sigma^2 \boldsymbol{I})} L(\boldsymbol{w} + \boldsymbol{\epsilon}_r). \tag{2}$$

Such expected loss objective can effectively smooth the loss landscape and thereby recover flat minima (Bisla et al., 2022).

The above two objectives resemble in formulation except that the maximum in (1) is replaced by an expectation in (2). Intuitively, the expectation could be viewed as a 'softer' version of the maximum. Möllenhoff & Khan (2023) demonstrates that the above two objectives can be bridged mathematically, leveraging the tools of Fenchel biconjugate in convex optimization (Hiriart-Urruty & Lemaréchal, 2004). Specifically, let $L^{\text{relaxed}}(\boldsymbol{w})$ be the Fenchel biconjugate of $L^{\text{Bayes}}(\boldsymbol{w})$ defined in the dual spaces of exponential-family distributions (Wainwright et al., 2008), which is a convex relaxation w.r.t. original Bayes objective. There exists an equivalence such that

$$\arg\min_{\boldsymbol{w}} L^{\text{SAM}}(\boldsymbol{w}) = \arg\min_{\boldsymbol{w}} L^{\text{relaxed}}(\boldsymbol{w}), \tag{3}$$

assuming the SAM-perturbation satisfies $\|\boldsymbol{\epsilon}_s\| = \rho$ at a stationary point.

4 Random Weight Perturbation v.s. Adversarial Weight Perturbation

Despite the theoretical connection established between the 'max-loss' and 'expected-loss' objectives, the performance of the latter still empirically lags behind the performance of the former, as the biconjugate function could not be attained in real neural network functions and there are gaps between the original objectives and its approximation. In this section, we work on a practical analysis for solving the above two objectives through the lens of weight perturbation.

Method	Perturbation Radius	Gradient Information	Computation	Time	Accuracy (%)
AWP	Small	Yes	2×	2×	77.15
RWP	Medium	No	1×	1×	76.77
ARWP	Medium	Yes	1×	1×	77.02
m-ARWP	Large	Yes	2×	1×	78.04

Table 1: An overall comparison of different methods. RWP and ARWP utilize much larger perturbation radius than AWP, while m-ARWP can utilize even larger perturbation radius due to the improved convergence. The "gradient information" denotes whether utilizing gradient information for generating weight perturbation. RWP and ARWP requires only half of computation budget than AWP, while m-ARWP is able to paralleling the computation of the two gradient steps to half the training time. For performance comparison on ImageNet with ResNet-50, RWP and variants can achieve much more efficient generalization improvement than AWP.

Adversarial Weight Perturbation (AWP). To optimize L^{SAM}, we first have to find the worst-case perturbations $\boldsymbol{\epsilon}_s^*$ for the max problem. Foret *et al.* (Foret et al., 2020) practically approximate (1) via the first-order expansion:

$$\boldsymbol{\epsilon}_s^* \approx \underset{\|\boldsymbol{\epsilon}_s\|_2 \leq \rho}{\arg\max}\, \boldsymbol{\epsilon}_s^\top \nabla_{\boldsymbol{w}} L(\boldsymbol{w}) = \rho \frac{\nabla_{\boldsymbol{w}} L(\boldsymbol{w})}{\|\nabla_{\boldsymbol{w}} L(\boldsymbol{w})\|_2}. \tag{4}$$

Then the gradient at the perturbed weight $\boldsymbol{w} + \boldsymbol{\epsilon}_s^*$ is computed for updating the model:

$$\nabla L^{\text{SAM}}(\boldsymbol{w}) \approx \nabla L(\boldsymbol{w})|_{\boldsymbol{w}+\boldsymbol{\epsilon}_s^*}. \tag{5}$$

Due to the two sequential gradient calculations involved for each iteration, the training speed of SAM is 2× that of regular SGD training.

Random Weight Perturbation (RWP). For optimizing L^{Bayes}, we similarly sample a random perturbation $\boldsymbol{\epsilon}_r$ from a given distribution for each iteration and calculate the gradient at the perturbed weight $\boldsymbol{w} + \boldsymbol{\epsilon}_r$ for updating the model:

$$\nabla L^{\text{Bayes}}(\boldsymbol{w}) \approx \nabla L(\boldsymbol{w})|_{\boldsymbol{w}+\boldsymbol{\epsilon}_r}. \tag{6}$$

Note that the selection of the distribution plays an crucial role in the effectiveness of RWP. For modern DNNs, the loss function does not change with parameter scaling when ReLU-nonlinearities and batch normalization (Ioffe & Szegedy, 2015) are applied. Hence, it is essential to consider the filter-wise structure. Following the approach in (Bisla et al., 2022), we practically generate the RWP from a filter-wise Gaussian distribution, i.e., $\boldsymbol{\epsilon}_r \sim \mathbb{N}\left(\mathbf{0}, \sigma^2 diag(\{\|\boldsymbol{w}^{(j)}\|^2\}_{j=1}^k)\right)$, with σ controlling the perturbation magnitude.

RWP requires much larger magnitude. As the precise gradient direction is known, AWP is much more "effective" at perturbing the model compared to RWP. Consequently, in order to achieve a similar level of perturbation strength, the magnitude of RWP needs to be considerably larger than that of AWP. We carry out comparative experiments using a model $\boldsymbol{w}^*$ that has been well-trained with SGD and apply different perturbation magnitudes for both RWP and AWP. As dipicted in Figure 1, to attain a similar expected perturbed training loss $\mathbb{E}\left[L(\boldsymbol{w}^* + \boldsymbol{\epsilon})\right]$ (we calculate the mean perturbed loss over the entire training set with a batch size of 256), the perturbation radius of RWP would need to be roughly two orders of magnitude larger than that of AWP. Such large perturbations can introduce instability in training and cause convergence issues that degrade the performance.

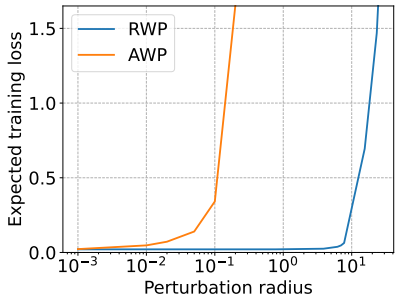

Figure 1: Expected training loss $\mathbb{E}[L(\boldsymbol{w}^* + \boldsymbol{\epsilon})]$ under different perturbation radii $\|\boldsymbol{\epsilon}\|_2$. The experiments employ a well-trained model $\boldsymbol{w}^*$ using SGD on CIFAR-10 with ResNet-18. Note that the x-axis is in logarithmic coordinates.

5 Improving Random Weight Perturbation

In this section, we propose to improve the performance of random weight perturbation from two primary perspectives. Firstly, we integrate the original loss objective to facilitate improved convergence. This allows more stable training and utilizing larger perturbation magnitude for better generalization performance. Secondly, we focus on refining weight perturbation generation by incorporating historical gradient information. This enables a more adaptive and effective perturbation generation process.

5.1 Improving Convergence by Incorporating Original Loss

We here first investigate the convergence properties of the following SGD optimization under RWP:

$$\boldsymbol{w}_{t+1} = \boldsymbol{w}_t - \gamma_t \nabla L_{\mathcal{B}}(\boldsymbol{w}_t + \boldsymbol{\epsilon}_r), \tag{7}$$

where $\mathcal{B}$ denotes the batch data. We first make some standard assumptions on smoothness and bounded variance of stochastic gradients, which are typical as in (Duchi et al., 2012; Ghadimi & Lan, 2013; Karimi et al., 2016; Andriushchenko & Flammarion, 2022; Jiang et al., 2023).

Assumption 1 (Bounded variance) *There exists a constant $M > 0$ for any data batch $\mathcal{B}$ such that*

$$\mathbb{E}\left[\|\nabla L_{\mathcal{B}}(\boldsymbol{w}) - \nabla L(\boldsymbol{w})\|_2^2\right] \leq M, \quad \forall \boldsymbol{w} \in \mathbb{R}^d. \tag{8}$$

Assumption 2 (β-smoothness) *Assume the loss function $L : \mathbb{R}^d \mapsto \mathbb{R}$ to be β-smooth. There exists $\beta > 0$ such that*

$$\|\nabla L(\boldsymbol{w}) - \nabla L(\boldsymbol{v})\|_2 \leq \beta \|\boldsymbol{w} - \boldsymbol{v}\|_2, \quad \forall \boldsymbol{w}, \boldsymbol{v} \in \mathbb{R}^d. \tag{9}$$

Theorem 1 (Convergence of RWP in non-convex setting) *Assume Assumption 1 and 2 hold. Let $\boldsymbol{\epsilon}_r \sim \mathcal{N}(0, \sigma^2 I_{d\times d})$ be the random perturbation and b be the batch size. Consider the sequence $(\boldsymbol{w}_t)_{t\in\mathbb{N}}$ generated by (7), with a stepsize satisfying $\gamma_t = \frac{\gamma_0}{\sqrt{t}}$ and $\gamma < \frac{1}{\beta}$. Then we have*

$$\frac{1}{T}\sum_{t=1}^{T} \mathbb{E}\|\nabla L(\boldsymbol{w}_t)\|^2 \leq \frac{2\left(\mathbb{E}[L(\boldsymbol{w}_0)] - \mathbb{E}[L(\boldsymbol{w}^*)]\right)}{\gamma_0\sqrt{T}} + (2\beta M + \beta^3\sigma^2 d)\gamma_0 \frac{\log T}{\sqrt{T}} + 2\beta^2\sigma^2 d. \tag{10}$$

We provide the proof in Appendix A and make several remarks: (1) Different from prior theoretical analysis (Andriushchenko & Flammarion, 2022; Mi et al., 2022) in SAM that assumes a decreasing magnitude on perturbation strength for achieving good convergence properties (e.g. $\rho_t = \frac{\rho_0}{\sqrt{t+1}}$ in Andriushchenko & Flammarion (2022)), we consider a more realistic setting with a non-decreasing σ that is adopted in practice. (2) There are three terms that upper bound the expected training loss. The first two terms decrease at a rate of $\mathcal{O}(\frac{1}{\sqrt{t}})$ and $\mathcal{O}(\frac{\log(t)}{\sqrt{t}})$, respectively, which is consistent with the convergence rate of regular SGD. $\beta^3\sigma^2 d$ is the additional variance term introduced by random weight perturbation. It can remain large when the perturbation radius ($\|\boldsymbol{\epsilon}_r\|$) is large, of which the expected radius is $\mathbb{E}[\|\boldsymbol{\epsilon}_r\|^2] = \sigma^2 d$, thereby slowing down convergence. The third term is a positive constant proportional to the perturbation magnitude σ^2, which prevents the effective reduction of the gradient norm beyond a certain point.

From the above convergence analysis, we know that the convergence of RWP is severely affected by the perturbation magnitude, which is substantially larger than AWP adopted in SAM (Foret et al., 2020) as demonstrated in Figure 1. This can cause slow and unstable convergence, which degrades the generalization performance. To improve the convergence of RWP, we propose to combine the original loss with the expected Bayes loss, i.e.,

$$L^{\mathrm{m}}(\boldsymbol{w}) = \lambda L^{\mathrm{Bayes}}(\boldsymbol{w}) + (1-\lambda) L(\boldsymbol{w}), \tag{11}$$

where $\lambda \in [0, 1]$ is a pre-given balance coefficient. The two loss terms in our ***mixed-RWP*** (m-RWP) objective are complementary to each other: the first $L^{\mathrm{Bayes}}(\boldsymbol{w})$ provides a smoothed landscape that biases the network

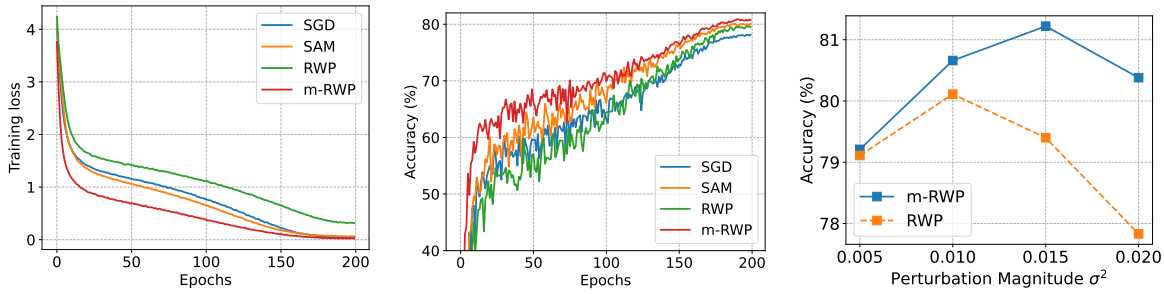

(a) (b) (c)

Figure 2: Training performance comparison of RWP and m-RWP. In (a) and (b), m-RWP significantly improve the convergence over RWP and leads to much better performance; and in (c), the improved convergence allows m-RWP to utilize larger perturbation magnitude, which also contributes to better generalization.

towards flat region, while the second $L(\boldsymbol{w})$ helps recover the necessary local information and better locates the minima that contributes to high performance. These two together could provide a both "local" and "global" viewing of the landscape — by optimizing $L^{\mathrm{m}}(\boldsymbol{w})$, a good solution can be expected.

In practical implementation, we adopt a specific procedure for optimizing the objective function $L^{\mathrm{Bayes}}(\boldsymbol{w})$ using RWP, i.e., in each training iteration, we sample one single random weight perturbation vector denoted as $\boldsymbol{\epsilon}_r$. To enhance the optimization process, we utilize two distinct batches of data, namely $\mathcal{B}_1$ and $\mathcal{B}_2$, for the two gradient steps involved. Note that this effectively enlarges the virtual batch size by a factor of two. The optimization process of our m-RWP can be formulated as follows:

$$\boldsymbol{w}_{t+1} = \boldsymbol{w}_t - \gamma_t \left[\lambda \nabla L_{\mathcal{B}_1}(\boldsymbol{w}_t + \boldsymbol{\epsilon}_r) + (1-\lambda)\nabla L_{\mathcal{B}_2}(\boldsymbol{w}_t)\right]. \tag{12}$$

In the following, we analyze the convergence properties of m-RWP with proof in Appendix B.

Theorem 2 (Convergence of m-RWP in non-convex setting) *Assume Assumption 1 and 2 hold. Let $\boldsymbol{\epsilon}_r \sim \mathcal{N}(0, \sigma^2 I_{d\times d})$ be the random perturbation and b be the batch size. Consider the sequence $(\boldsymbol{w}_t)_{t\in\mathbb{N}}$ generated by (12), with a stepsize satisfying $\gamma_t = \frac{\gamma_0}{\sqrt{t}}$ and $\gamma < \frac{1}{\beta}$. Then we have*

$$\frac{1}{T}\sum_{t=1}^{T}\mathbb{E}\|\nabla L(\boldsymbol{w}_t)\|^2 \leq \frac{2\left(\mathbb{E}[L(\boldsymbol{w}_0)] - \mathbb{E}[L(\boldsymbol{w}^*)]\right)}{\gamma_0\sqrt{T}} + \left[2\beta M(2\lambda^2 - 2\lambda + 1) + \beta^3\lambda^2\sigma^2 d\right]\gamma_0\frac{\log T}{\sqrt{T}} + 2\beta^2\lambda^2\sigma^2 d.$$

Improved Convergence. Compared to the convergence properties of RWP stated in Theorem 1, m-RWP offers immediate improvements in two aspects. First, it reduces the variance term introduced by random weight perturbation ($\beta^3\lambda^2 d\gamma_0\frac{\log T}{\sqrt{T}}$) and the positive constant term ($2\beta^2\sigma^2 d$) by a factor of λ^2. Second, m-RWP allows the use of two different data batches to compute the two gradient steps. This effectively doubles the batch size and thus reduces the gradient variance term ($2\beta M\gamma_0\frac{\log T}{\sqrt{T}}$) by a factor of $2\lambda^2 - 2\lambda + 1$. As a result, the convergence is significantly improved.

Utilizing Larger Perturbation Magnitude. With the improved convergence achieved by m-RWP, the utilization of larger perturbation magnitudes becomes feasible, resulting in flatter minima and improved performance. This effect is illustrated in Figure 2, where it can be observed that m-RWP exhibits significantly enhanced convergence compared to RWP. Consequently, the ability to employ larger perturbation magnitudes enables m-RWP to achieve substantially better performance.

Efficient Parallel Training. Both SAM and m-RWP indeed involve two gradient steps for each iteration: $\nabla L(\boldsymbol{w})$ and $\nabla L(\boldsymbol{w} + \boldsymbol{\epsilon})$. However, the key distinction lies in the separability of these steps. In m-RWP, they are separable, and can be calculated independently and in parallel, whereas, in SAM, they need to be computed sequentially. This parallel computing capability of m-RWP allows for a halving of the training time, making it a highly efficient approach for large-scale problems.

5.2 Adaptive Random Weight Perturbation Generation

One limitation of previous methods for generating RWP is their exclusive reliance on weight norm, without utilizing any gradient information. This approach creates a disconnect between perturbation generation and the actual loss objective, resulting in overly "rough" perturbations.

Despite that for the efficiency considerations, we can not adopt an additional gradient step to assist the generation of RWP, the historical perturbed gradients are available and can be leveraged. We thus propose to utilize the historical gradient to better guide the generation of RWP. To achieve this, we employ an element-wise scaling of the gradient, taking into account the historical running sum of squares in each dimension. It is important to note that this technique is widely used in adaptive gradient descent optimizers such as Adam (Kingma & Ba, 2015) and RMSprop (Tieleman et al., 2012). The generation form of our proposed method, called Adaptive Random Weight Perturbation (ARWP), is as follows:

$$\boldsymbol{\epsilon}_{r,t} \sim \mathbb{N}\left(\mathbf{0}, \frac{\sigma^2 \boldsymbol{I}}{\sqrt{1+\eta\sum_{i=1}^{t-1}\beta^{t-i-1}\boldsymbol{g}_i^2}}\right), \tag{13}$$

where η and β are two hyper-parameters. The rationale behind our generation approach is to move away from assigning a uniform perturbation magnitude (σ) to all parameters. Instead, we aim to introduce an adaptive perturbation strength based on the historical perturbation gradients. The idea is that if the historical gradients are large, we want to assign a smaller perturbation magnitude. By incorporating this adaptability, we can tailor the perturbation magnitudes to the specific characteristics of each parameter. This allows us to account for variations in sensitivity and importance across different dimensions, leading to a more adaptive and effective generation of perturbations. Then combing with the filter-wise perturbation generation techniques from Bisla et al. (2022), our generation approach can be expressed as follows:

$$\boldsymbol{\epsilon}_{r,t} \sim \mathbb{N}\left(\mathbf{0}, \frac{\sigma^2 diag(\{\|\boldsymbol{w}_t^{(j)}\|^2\}_{j=1}^k)}{\sqrt{1+\eta\sum_{i=1}^{t-1}\beta^{t-i-1}diag(\{\|\boldsymbol{g}_i^{(j)}\|^2\}_{j=1}^k)}}\right). \tag{14}$$

Then combining the mixed loss objective in Eqn. (11), we propose our m-ARWP approach, which takes the same computational cost as SAM while being capable of halving the training time through parallel computation of the two gradient steps.

6 Experiments

In this section, we present extensive experimental results to demonstrate the efficiency and effectiveness of our proposed methods. We begin by introducing the experimental setup and then evaluate the performance over three standard benchmark datasets: CIFAR-10, CIFAR-100 and ImageNet. We also conduct ablation studies on the hyper-parameters and visualize the loss landscape to provide further insights.

6.1 Results

Datasets & Models. We experiment over three benchmark image classification tasks: CIFAR-10, CIFAR-100 (Krizhevsky & Hinton, 2009), and ImageNet (Deng et al., 2009). For CIFAR, we apply standard random horizontal flipping, cropping, normalization, and Cutout augmentation (DeVries & Taylor, 2017) (except for ViT, for which we use RandAugment (Cubuk et al., 2020)). For ImageNet, we apply basic data preprocessing and augmentation following the public Pytorch example (Paszke et al., 2017). We evaluate across a variety of representative architectures, including VGG (Simonyan & Zisserman, 2014), ResNet (He et al., 2016), WideResNet (Zagoruyko & Komodakis, 2016), and ViT (Dosovitskiy et al., 2021).

Training Settings. We compare the performance of five training methods: SGD, SAM, RWP, ARWP, and m-ARWP. It is worth noting that SGD, RWP, and ARWP share the same computation (1×), while SAM and m-ARWP require twice the computational resources (2×). For CIFAR experiments, we set the training epochs to 200 with batch size 256, momentum 0.9, and weight decay 0.001 (Du et al., 2022a; Zhao

et al., 2022a), keeping the same among all methods for a fair comparison (except for ViT, we adopt a longer training schedule and provide the details in Appendix C). We set ρ for SAM as 0.05 for CIFAR-10 and 0.10 for CIFAR-100 as in (Foret et al., 2020; Kwon et al., 2021). For RWP and ARWP, we set $\sigma = 0.01$ for both CIFAR-10/100 as it gives the optimal performance. We also adopt a cosine increasing schedule for σ as described in (Bisla et al., 2022). For m-ARWP, we use $\sigma = 0.015$ and $\lambda = 0.5$ as it gives moderately good performance across different models. We set $\eta = 0.1$ and $\beta = 0.99$ as default choice. For ImageNet experiments, we set the training epochs to 90 with batch size 256, weight decay 0.0001, and momentum 0.9. We use $\rho = 0.05$ for SAM following (Foret et al., 2020; Kwon et al., 2021), $\sigma = 0.003$ for RWP and ARWP, and $\sigma = 0.005$, $\lambda = 0.5$ for m-ARWP. We employ m-sharpness with $m = 128$ for SAM as in (Foret et al., 2020; Kwon et al., 2021). For all experiments, we adopt cosine learning rate decay (Loshchilov & Hutter, 2016) with an initial learning rate of 0.1 and record the final model performance on the test set. Mean and standard deviation are calculated over three independent trials.

Table 2: Results on CIFAR-10/100. We set the computation (FLOPs) and training time of SGD as 1×. The best accuracy is in bold and the second best is underlined.

Model	Method	CIFAR-10	CIFAR-100	FLOPs	Time
VGG16-BN	SGD	94.96±0.15	75.43±0.29	1×	1×
	SAM	<u>95.43</u>±0.11	76.74±0.22	2×	2×
	RWP	94.97±0.07	76.56±0.10	1×	1×
	ARWP	95.07±0.23	<u>77.07</u>±0.21	1×	1×
	m-ARWP	**95.61**±0.23	**77.98**±0.19	2×	1×
ResNet-18	SGD	96.10±0.08	78.10±0.39	1×	1×
	SAM	<u>96.50</u>±0.08	80.22±0.23	2×	2×
	RWP	96.01±0.31	80.21±0.14	1×	1×
	ARWP	96.30±0.03	<u>80.71</u>±0.24	1×	1×
	m-ARWP	**96.68**±0.17	**81.38**±0.12	2×	1×
WRN-28-10	SGD	96.85±0.05	82.51±0.24	1×	1×
	SAM	**97.37**±0.02	<u>84.44</u>±0.03	2×	2×
	RWP	96.73±0.12	83.67±0.14	1×	1×
	ARWP	96.89±0.11	83.96±0.09	1×	1×
	m-ARWP	<u>97.27</u>±0.09	**84.56**±0.12	2×	1×
ViT-S	Adam	86.60±0.03	63.66±0.28	1×	1×
	SAM	<u>87.48</u>±0.28	<u>64.83</u>±0.24	2×	2×
	RWP	86.53±0.04	63.67±0.41	1×	1×
	ARWP	86.88±0.09	64.12±0.22	1×	1×
	m-ARWP	**88.18**±0.19	**66.13**±0.03	2×	1×

CIFAR. We begin by focusing on the CIFAR-10 and CIFAR-100 datasets. We evaluate the final test accuracy, total computation (in FLOPs), and training time for different methods. Detailed comparisons are presented in Table 2. We observe that ARWP consistently improves the performance RWP by 0.1-0.3% on CIFAR-10 and 0.3-0.5% on CIFAR-100, and m-ARWP consistently outperforms ARWP, improving performance by 1.6% on CIFAR-10 and 3.1% on CIFAR-100, confirming the effectiveness of our improvements on enhancing generalization. It is also worth mentioning that ARWP can achieve competitive, and sometimes even better, generalization performance compared to SAM, particularly with VGG16-BN (+0.3%) and ResNet-18 (+0.5%) models on CIFAR-100. Remarkably, ARWP achieves this with only half of the computation required by SAM. Additionally, m-ARWP outperforms SAM in most cases on CIFAR-10, and achieves improvements ranging from 0.1% to 1.3% on CIFAR-100. Lastly, it is important to note that although both SAM and m-ARWP require twice the computation of SGD, the training time of m-RWP can be reduced by half compared to SAM through parallel computing. This reduction in training time is a valuable advantage of m-ARWP.

ImageNet. Next, we evaluate our proposed methods on ImageNet dataset, which has a substantially larger scale than CIFAR. We evaluate over three different architectures, namely VGG16-BN, ResNet-18,

and ResNet-50, and present the results in Table 3. We observe that ARWP can achieve very competitive performance against SAM. For instance, with ResNet-18, ARWP achieves an accuracy of 70.71% compared to SAM's 70.77%, while with ResNet-50, ARWP achieves 77.02% accuracy compared to SAM's 77.15%. Notably, ARWP accomplishes this while requiring only half of the computational resources. Furthermore, m-ARWP significantly outperforms SAM, achieving 75.79% accuracy (+1.14%) with VGG16-BN, 71.58% accuracy (+0.81%) with ResNet-18, and 78.04% accuracy (+0.89%) with ResNet-50. We note that models trained on ImageNet are typically under-trained. Therefore, the improved convergence of m-ARWP offers even more significant advantages over SAM. Moreover, the capability of parallel computing in m-ARWP is especially advantageous as the 2× longer training time in SAM would be prohibitively slow for large-scale problems.

Table 3: Results on ImageNet. We set the computation (FLOPs) and training time of SGD as 1×. The best accuracy is in bold and the second best is underlined.

Model	Training	Top-1 Acc.	Top-5 Acc.	FLOPs	Time
VGG16-BN	SGD	73.11	91.12	1×	1×
	SAM	<u>74.65</u>	<u>92.21</u>	2×	2×
	RWP	74.01	91.66	1×	1×
	ARWP	74.28	91.96	1×	1×
	m-ARWP	**75.79**	**92.92**	2×	1×
ResNet-18	SGD	70.32	89.66	1×	1×
	SAM	<u>70.77</u>	<u>89.83</u>	2×	2×
	RWP	70.46	89.71	1×	1×
	ARWP	70.71	89.79	1×	1×
	m-ARWP	**71.58**	**90.31**	2×	1×
ResNet-50	SGD	76.62	93.24	1×	1×
	SAM	<u>77.15</u>	<u>93.55</u>	2×	2×
	RWP	76.77	93.27	1×	1×
	ARWP	77.02	93.34	1×	1×
	m-ARWP	**78.04**	**93.91**	2×	1×

6.2 Ablation Study and Visualization

Impact of different data batches. We conducted a further investigation into the impact of using the same or different data batches for the two gradient steps in m-ARWP and SAM. The results are presented in Table 4, and we made the following observations. For m-ARWP, both choices of using the same or different data batches yield comparable performance, with the use of different batches resulting in a slightly better performance. On the other hand, for SAM, the two approaches yield starkly different results. Adopting different data batches for the adversarial attack and gradient propagation in SAM would undesirably degrade its generalization performance to that of plain SGD. This finding suggests that applying the same data batch for adversarial attack and gradient propagation is a crucial aspect for SAM's generalization improvement. We attribute this difference to the unique characteristic of AWP in SAM, which is specific to a particular batch of data. The perturbation computed over one batch in SAM can degenerate into meaningless noise when applied to another batch. In contrast, the perturbation used in m-ARWP is not associated with specific data instances, allowing for the use of different data batches to accelerate convergence with better efficiency.

Table 4: Effects of same/different data batches for two gradient steps. The experiments are conducted on CIFAR-100 with ResNet-18.

Training	Same	Different
SAM	80.22±0.23	78.30±0.11 (↓ 1.92)
m-ARWP	81.14±0.10	81.38±0.12 (↑ 0.24)

Sensitivity of hyper-parameters. There are four hyper-parameters involved in our approaches, η and β in ARWP, and additionally λ and σ in m-ARWP. We note that for the first three hyper-parameters, we use default values as $\eta = 1$, $\beta = 0.99$, $\lambda = 0.5$ across different experiments and only σ needs to be tuned, thus

virtually having the same number of hyper-parameters as SAM and RWP. To better understand their effects on performance, we test the performance under different choices of values. Specifically, we test on CIFAR-10/100 datasets with ResNet-18, and vary η in $\{0.01, 0.1, 1\}$, β in $\{0.9, 0.99, 0.999\}$, σ in $\{0.005, 0.01, 0.015, 0.02\}$ and λ in $\{0.1, 0.3, 0.5, 0.7, 0.9\}$. The results are in Figure 3. We observe that $\eta = 0.1$, $\beta = 0.99$, $\sigma = 0.015$, and $\lambda = 0.5$ are a robust choice that achieves moderately good performance on both CIFAR-10 and CIFAR-100.

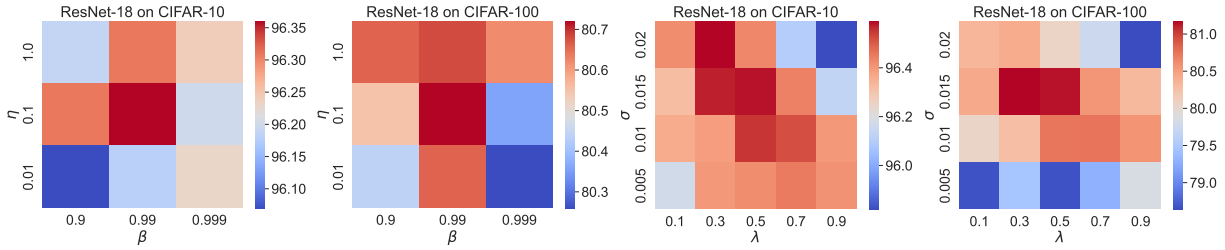

(a) ARWP (b) m-ARWP, $\eta = 0.1$, $\beta = 0.99$

Figure 3: Performance under various hyper-parameter configurations.

Loss landscape and Hessian spectrum. Finally, we compare the loss landscape and Hessian spectrum of SGD, RWP, ARWP, SAM, and m-ARWP. Following the plotting technique in (Li et al., 2018), we uniformly sample 50×50 grid points in the range of $[-1, 1]$ from random "filter-normalized" direction (Li et al., 2018), and for Hessian spectrum, we approximate it using the Lanczos algorithm (Ghorbani et al., 2019). In Figure 4, we observe that RWP, ARWP, SAM, and m-ARWP all achieve flatter loss landscape and smaller dominant eigenvalue (λ_1) compared to SGD. Additionally, ARWP demonstrates improved flatness and dominant eigenvalue compared to RWP. Moreover, m-ARWP exhibits even better flatness and a smaller dominant eigenvalue than SAM. Interestingly, from the perspective of the loss landscape, RWP and ARWP appear to have flatter landscapes compared to SAM and m-ARWP. However, they exhibit much larger Hessian dominant eigenvalues and worse generalization performance. This discrepancy may be attributed to the fact that the minima found by RWP and ARWP may not converge well and are even "over-smoothed" due to the large perturbation radius involved. Conversely, with the improved convergence of m-ARWP, we were able to reach a more precise minimum with better generalization performance.

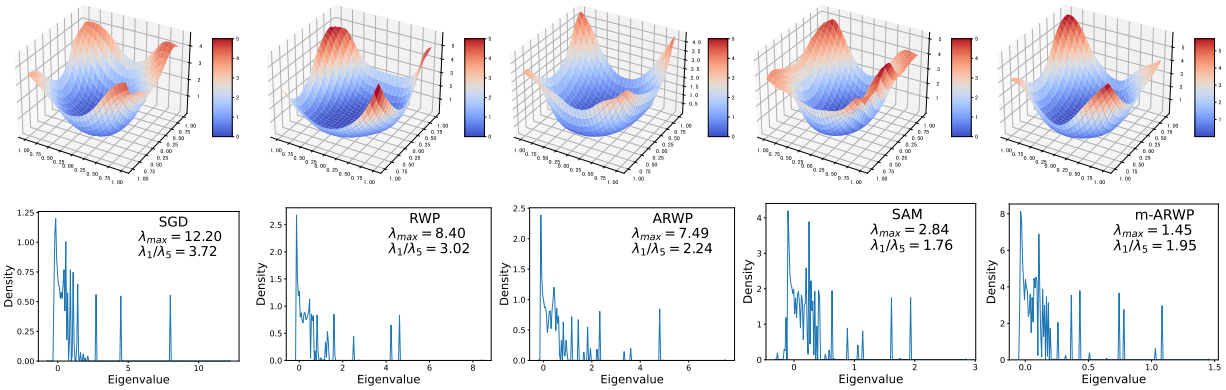

Figure 4: Loss landscape (**Up**) and the corresponding Hessian spectrum visualization (**Down**) of different methods. Models are trained on CIFAR-10 with ResNet-18.

7 Conclusion

In this work, we revisit the use of random weight perturbation for improving generalization performance. From the basic standpoint that RWP is more computationally efficient than AWP but requires a much larger perturbation radius, we improve RWP from the perspective of convergence and also introduce an adaptive strategy that utilizes historical gradient information for better perturbation generation. Extensive experiments on various architectures and tasks demonstrate that our improved RWP is able to achieve more efficient generalization improvement than AWP, especially on large-scale problems.

References

Maksym Andriushchenko and Nicolas Flammarion. Towards understanding sharpness-aware minimization. In *International Conference on Machine Learning (ICML)*, 2022.

Devansh Bisla, Jing Wang, and Anna Choromanska. Low-pass filtering sgd for recovering flat optima in the deep learning optimization landscape. In *International Conference on Artificial Intelligence and Statistics (AISTATIS)*, 2022.

Ekin D Cubuk, Barret Zoph, Jonathon Shlens, and Quoc V Le. Randaugment: Practical automated data augmentation with a reduced search space. In *Proceedings of the IEEE/CVF Conference on Computer Vision and Pattern Recognition Workshops*, pp. 702–703, 2020.

Jia Deng, Wei Dong, Richard Socher, Li-Jia Li, Kai Li, and Li Fei-Fei. Imagenet: A large-scale hierarchical image database. In *Proceedings of the IEEE Conference on Computer Vision and Pattern Recognition (CVPR)*, 2009.

Terrance DeVries and Graham W Taylor. Improved regularization of convolutional neural networks with cutout. *arXiv preprint arXiv:1708.04552*, 2017.

Laurent Dinh, Razvan Pascanu, Samy Bengio, and Yoshua Bengio. Sharp minima can generalize for deep nets. In *International Conference on Machine Learning (ICML)*, 2017.

Alexey Dosovitskiy, Lucas Beyer, Alexander Kolesnikov, Dirk Weissenborn, Xiaohua Zhai, Thomas Unterthiner, Mostafa Dehghani, Matthias Minderer, Georg Heigold, Sylvain Gelly, et al. An image is worth 16x16 words: Transformers for image recognition at scale. In *International Conference on Learning Representations (ICLR)*, 2021.

Jiawei Du, Hanshu Yan, Jiashi Feng, Joey Tianyi Zhou, Liangli Zhen, Rick Siow Mong Goh, and Vincent YF Tan. Efficient sharpness-aware minimization for improved training of neural networks. In *International Conference on Learning Representations (ICLR)*, 2022a.

Jiawei Du, Daquan Zhou, Jiashi Feng, Vincent YF Tan, and Joey Tianyi Zhou. Sharpness-aware training for free. In *Advances in Neural Information Processing Systems (NeurIPS)*, 2022b.

John C Duchi, Peter L Bartlett, and Martin J Wainwright. Randomized smoothing for stochastic optimization. *SIAM Journal on Optimization*, 22(2):674–701, 2012.

Pierre Foret, Ariel Kleiner, Hossein Mobahi, and Behnam Neyshabur. Sharpness-aware minimization for efficiently improving generalization. In *International Conference on Learning Representations (ICLR)*, 2020.

Saeed Ghadimi and Guanghui Lan. Stochastic first-and zeroth-order methods for nonconvex stochastic programming. *SIAM Journal on Optimization*, 23(4):2341–2368, 2013.

Behrooz Ghorbani, Shankar Krishnan, and Ying Xiao. An investigation into neural net optimization via hessian eigenvalue density. In *International Conference on Machine Learning*, 2019.

Kaiming He, Xiangyu Zhang, Shaoqing Ren, and Jian Sun. Deep residual learning for image recognition. In *Proceedings of the IEEE Conference on Computer Vision and Pattern Recognition (CVPR)*, 2016.

Jean-Baptiste Hiriart-Urruty and Claude Lemaréchal. *Fundamentals of convex analysis*. Springer Science & Business Media, 2004.

Sepp Hochreiter and Jürgen Schmidhuber. Simplifying neural nets by discovering flat minima. In *Advances in Neural Information Processing Systems (NeurIPS)*, 1994.

Sepp Hochreiter and Jürgen Schmidhuber. Flat minima. *Neural computation*, 1997.

Sergey Ioffe and Christian Szegedy. Batch normalization: Accelerating deep network training by reducing internal covariate shift. In *International Conference on Machine Learning (ICML)*, 2015.

Pavel Izmailov, Dmitrii Podoprikhin, Timur Garipov, Dmitry Vetrov, and Andrew Gordon Wilson. Averaging weights leads to wider optima and better generalization. *arXiv preprint arXiv:1803.05407*, 2018.

Weisen Jiang, Hansi Yang, Yu Zhang, and James Kwok. An adaptive policy to employ sharpness-aware minimization. In *International Conference on Learning Representations (ICLR)*, 2023.

Yiding Jiang*, Behnam Neyshabur*, Hossein Mobahi, Dilip Krishnan, and Samy Bengio. Fantastic generalization measures and where to find them. In *International Conference on Learning Representations (ICLR)*, 2020.

Chi Jin, Praneeth Netrapalli, Rong Ge, Sham M Kakade, and Michael I Jordan. On nonconvex optimization for machine learning: Gradients, stochasticity, and saddle points. *Journal of the ACM (JACM)*, 2021.

Hamed Karimi, Julie Nutini, and Mark Schmidt. Linear convergence of gradient and proximal-gradient methods under the polyak-łojasiewicz condition. In *Joint European Conference on Machine Learning and Knowledge Discovery in Databases*, 2016.

Nitish Shirish Keskar, Dheevatsa Mudigere, Jorge Nocedal, Mikhail Smelyanskiy, and Ping Tak Peter Tang. On large-batch training for deep learning: Generalization gap and sharp minima. In *International Conference on Learning Representations (ICLR)*, 2017.

Minyoung Kim, Da Li, Shell X Hu, and Timothy Hospedales. Fisher sam: Information geometry and sharpness aware minimisation. In *International Conference on Machine Learning (ICML)*, 2022.

Diederik P. Kingma and Jimmy Lei Ba. Adam: A method for stochastic optimization. In *International Conference on Learning Representations (ICLR)*, 2015.

Alexander Kolesnikov, Lucas Beyer, Xiaohua Zhai, Joan Puigcerver, Jessica Yung, Sylvain Gelly, and Neil Houlsby. Big transfer (bit): General visual representation learning. In *European conference on computer vision (ECCV)*, 2020.

Alex Krizhevsky and Geoffrey Hinton. Learning multiple layers of features from tiny images. *Technical Report*, 2009.

Jungmin Kwon, Jeongseop Kim, Hyunseo Park, and In Kwon Choi. Asam: Adaptive sharpness-aware minimization for scale-invariant learning of deep neural networks. In *International Conference on Machine Learning (ICML)*, 2021.

Hao Li, Zheng Xu, Gavin Taylor, Christoph Studer, and Tom Goldstein. Visualizing the loss landscape of neural nets. In *Advances in Neural Information Processing Systems (NeurIPS)*, 2018.

Yong Liu, Siqi Mai, Xiangning Chen, Cho-Jui Hsieh, and Yang You. Towards efficient and scalable sharpness-aware minimization. In *Proceedings of the IEEE/CVF International Conference on Computer Vision (CVPR)*, 2022a.

Yong Liu, Siqi Mai, Minhao Cheng, Xiangning Chen, Cho-Jui Hsieh, and Yang You. Random sharpness-aware minimization. In *Advances in Neural Information Processing Systems (NeurIPS)*, 2022b.

Ze Liu, Yutong Lin, Yue Cao, Han Hu, Yixuan Wei, Zheng Zhang, Stephen Lin, and Baining Guo. Swin transformer: Hierarchical vision transformer using shifted windows. In *Proceedings of the IEEE/CVF International Conference on Computer Vision (CVPR)*, 2021.

Ilya Loshchilov and Frank Hutter. Sgdr: Stochastic gradient descent with warm restarts. *arXiv preprint arXiv:1608.03983*, 2016.

Peng Mi, Li Shen, Tianhe Ren, Yiyi Zhou, Xiaoshuai Sun, Rongrong Ji, and Dacheng Tao. Make sharpness-aware minimization stronger: A sparsified perturbation approach. *arXiv preprint arXiv:2210.05177*, 2022.

Thomas Möllenhoff and Mohammad Emtiyaz Khan. SAM as an optimal relaxation of Bayes. In *International Conference on Learning Representations (ICLR)*, 2023. URL https://openreview.net/forum?id=k4fevFqSQcX.

Behnam Neyshabur, Srinadh Bhojanapalli, David McAllester, and Nati Srebro. Exploring generalization in deep learning. In *Advances in Neural Information Processing Systems (NeurIPS)*, 2017.

Adam Paszke, Sam Gross, Soumith Chintala, Gregory Chanan, Edward Yang, Zachary DeVito, Zeming Lin, Alban Desmaison, Luca Antiga, and Adam Lerer. Automatic differentiation in pytorch. 2017.

Alec Radford, Jong Wook Kim, Chris Hallacy, Aditya Ramesh, Gabriel Goh, Sandhini Agarwal, Girish Sastry, Amanda Askell, Pamela Mishkin, Jack Clark, et al. Learning transferable visual models from natural language supervision. In *International Conference on Machine Learning (ICML)*, 2021.

Karen Simonyan and Andrew Zisserman. Very deep convolutional networks for large-scale image recognition. *arXiv preprint arXiv:1409.1556*, 2014.

Christian Szegedy, Vincent Vanhoucke, Sergey Ioffe, Jon Shlens, and Zbigniew Wojna. Rethinking the inception architecture for computer vision. In *Proceedings of the IEEE Conference on Computer Vision and Pattern Recognition (CVPR)*, 2016.

Mingxing Tan and Quoc Le. Efficientnet: Rethinking model scaling for convolutional neural networks. In *International Conference on Machine Learning (ICML)*, 2019.

Tijmen Tieleman, Geoffrey Hinton, et al. Lecture 6.5-rmsprop: Divide the gradient by a running average of its recent magnitude. *COURSERA: Neural networks for machine learning*, 4(2):26–31, 2012.

Martin J Wainwright, Michael I Jordan, et al. Graphical models, exponential families, and variational inference. *Foundations and Trends® in Machine Learning*, 1(1–2):1–305, 2008.

Ziqiao Wang and Yongyi Mao. On the generalization of models trained with sgd: Information-theoretic bounds and implications. In *International Conference on Learning Representations (ICLR)*, 2021.

Wei Wen, Yandan Wang, Feng Yan, Cong Xu, Chunpeng Wu, Yiran Chen, and Hai Li. Smoothout: Smoothing out sharp minima to improve generalization in deep learning. *arXiv preprint arXiv:1805.07898*, 2018.

Sergey Zagoruyko and Nikos Komodakis. Wide residual networks. In Richard C. Wilson, Edwin R. Hancock, and William A. P. Smith (eds.), *British Machine Vision Conference (BMVC)*, 2016.

Hongyi Zhang, Moustapha Cisse, Yann N Dauphin, and David Lopez-Paz. mixup: Beyond empirical risk minimization. In *International Conference on Learning Representations (ICLR)*, 2018.

Michael Zhang, James Lucas, Jimmy Ba, and Geoffrey E Hinton. Lookahead optimizer: k steps forward, 1 step back. In *Advances in Neural Information Processing Systems (NeurIPS)*, 2019.

Yang Zhao, Hao Zhang, and Xiuyuan Hu. Penalizing gradient norm for efficiently improving generalization in deep learning. In *International Conference on Machine Learning (ICML)*, 2022a.

Yang Zhao, Hao Zhang, and Xiuyuan Hu. SS-SAM: Stochastic scheduled sharpness-aware minimization for efficiently training deep neural networks. *arXiv preprint arXiv:2203.09962*, 2022b.

Yaowei Zheng, Richong Zhang, and Yongyi Mao. Regularizing neural networks via adversarial model perturbation. In *Proceedings of the IEEE Conference on Computer Vision and Pattern Recognition (CVPR)*, 2021.

Mo Zhou, Tianyi Liu, Yan Li, Dachao Lin, Enlu Zhou, and Tuo Zhao. Toward understanding the importance of noise in training neural networks. In *International Conference on Machine Learning (ICML)*, 2019.

Juntang Zhuang, Boqing Gong, Liangzhe Yuan, Yin Cui, Hartwig Adam, Nicha Dvornek, Sekhar Tatikonda, James Duncan, and Ting Liu. Surrogate gap minimization improves sharpness-aware training. In *International Conference on Learning Representations (ICLR)*, 2022.

A Proof of Theorem 1

Proof Denote $\boldsymbol{w}_{t+1/2} = \boldsymbol{w}_t + \boldsymbol{\epsilon}_{r,t}$. From Assumption 1, it follows that

$$
\begin{aligned}
L(\boldsymbol{w}_{t+1}) \leq & L(\boldsymbol{w}_t) + \nabla L(\boldsymbol{w}_t)^\top (\boldsymbol{w}_{t+1} - \boldsymbol{w}_t) + \frac{\beta}{2}\|\boldsymbol{w}_{t+1} - \boldsymbol{w}_t\|^2 && (15)\\
= & L(\boldsymbol{w}_t) - \gamma_t \nabla L(\boldsymbol{w}_t)^\top \nabla L_{\mathcal{B}}(\boldsymbol{w}_{t+1/2}) + \frac{\gamma_t^2 \beta}{2}\|\nabla L_{\mathcal{B}}(\boldsymbol{w}_{t+1/2})\|^2 && (16)\\
= & L(\boldsymbol{w}_t) - \gamma_t \nabla L(\boldsymbol{w}_t)^\top \nabla L_{\mathcal{B}}(\boldsymbol{w}_{t+1/2}) \\
& + \frac{\gamma_t^2 \beta}{2}\left(\|\nabla L_{\mathcal{B}}(\boldsymbol{w}_{t+1/2}) - \nabla L(\boldsymbol{w}_t)\|^2 - \|\nabla L(\boldsymbol{w}_t)\|^2 + 2\nabla L(\boldsymbol{w}_t)^\top \nabla L_{\mathcal{B}}(\boldsymbol{w}_{t+1/2})\right) && (17)\\
= & L(\boldsymbol{w}_t) - \frac{\gamma_t^2 \beta}{2}\|\nabla L(\boldsymbol{w}_t)\|^2 + \frac{\gamma_t^2 \beta}{2}\|\nabla L_{\mathcal{B}}(\boldsymbol{w}_{t+1/2}) - \nabla L(\boldsymbol{w}_t)\|^2 \\
& - (1 - \beta\gamma_t)\gamma_t \nabla L(\boldsymbol{w}_t)^\top \nabla L_{\mathcal{B}}(\boldsymbol{w}_{t+1/2}) && (18)\\
\leq & L(\boldsymbol{w}_t) - \frac{\gamma_t^2 \beta}{2}\|\nabla L(\boldsymbol{w}_t)\|^2 + \gamma_t^2 \beta \|\nabla L_{\mathcal{B}}(\boldsymbol{w}_{t+1/2}) - \nabla L(\boldsymbol{w}_{t+1/2})\|^2 \\
& + \gamma_t^2 \beta \|\nabla L(\boldsymbol{w}_{t+1/2}) - \nabla L(\boldsymbol{w}_t)\|^2 - (1 - \beta\gamma_t)\gamma_t \nabla L(\boldsymbol{w}_t)^\top \nabla L_{\mathcal{B}}(\boldsymbol{w}_{t+1/2}). && (19)
\end{aligned}
$$

The last step using the fact that $\|a - b\|^2 \leq 2\|a - c\|^2 + 2\|c - b\|^2$. Then taking the expectation on both sides gives:

$$
\mathbb{E}[L(\boldsymbol{w}_{t+1})] \leq \mathbb{E}[L(\boldsymbol{w}_t)] - \frac{\gamma_t^2 \beta}{2}\|\nabla L(\boldsymbol{w}_t)\|^2 + \gamma_t^2 \beta M + \gamma_t^2 \beta^3 \sigma^2 d - (1 - \beta\gamma_t)\gamma_t \nabla L(\boldsymbol{w}_t)^\top \nabla L_{\mathcal{B}}(\boldsymbol{w}_{t+1/2}). \quad (20)
$$

For the last term, we have:

$$
\begin{aligned}
\mathbb{E}[\nabla L(\boldsymbol{w}_t)^\top \nabla L_{\mathcal{B}}(\boldsymbol{w}_{t+1/2})] = & \mathbb{E}\left[\nabla L(\boldsymbol{w}_t)^\top \left(\nabla L_{\mathcal{B}}(\boldsymbol{w}_{t+1/2}) - \nabla L_{\mathcal{B}}(\boldsymbol{w}_t) + \nabla L_{\mathcal{B}}(\boldsymbol{w}_t)\right)\right] \\
= & \mathbb{E}\left[\|\nabla L(\boldsymbol{w}_t)\|^2\right] + \mathcal{C}.
\end{aligned} \quad (21)
$$

where $\mathcal{C} = \mathbb{E}\left[\nabla L(\boldsymbol{w}_t)^\top \left(\nabla L_{\mathcal{B}}(\boldsymbol{w}_{t+1/2}) - \nabla L_{\mathcal{B}}(\boldsymbol{w}_t)\right)\right]$. Using the Cauchy-Schwarz inequality, we have

$$
\begin{aligned}
\mathcal{C} \leq & \mathbb{E}\left[\frac{1}{2}\|\nabla L(\boldsymbol{w}_t)\|^2 + \frac{1}{2}\|\nabla L(\boldsymbol{w}_{t+1/2}) - \nabla L(\boldsymbol{w}_t)\|^2\right] \\
\leq & \frac{1}{2}\mathbb{E}\|\nabla L(\boldsymbol{w}_t)\|^2 + \frac{\beta^2 \sigma^2 d}{2}.
\end{aligned} \quad (22)
$$

Plugging Eqn. (21) and (22) into Eqn. (20), we obtain:

$$
\begin{aligned}
\mathbb{E}[L(\boldsymbol{w}_{t+1})] \leq & \mathbb{E}[L(\boldsymbol{w}_t)] - \frac{\gamma_t^2 \beta}{2}\mathbb{E}\|\nabla L(\boldsymbol{w}_t)\|^2 + \gamma_t^2 \beta M + \gamma_t^2 \beta^3 \sigma^2 d - (1 - \beta\gamma_t)\gamma_t \mathbb{E}\left[\|\nabla L(\boldsymbol{w}_t)\|^2\right] \\
& + (1 - \beta\gamma_t)\gamma_t \left(\frac{1}{2}\mathbb{E}\|\nabla L(\boldsymbol{w}_t)\|^2 + \frac{\beta^2 \sigma^2 d}{2}\right) && (23)\\
\leq & \mathbb{E}[L(\boldsymbol{w}_t)] - \frac{\gamma_t}{2}\mathbb{E}\|\nabla L(\boldsymbol{w}_t)\|^2 + \gamma_t^2 \beta M + \frac{1}{2}(1 + \beta\gamma_t)\gamma_t \beta^2 \sigma^2 d && (24)
\end{aligned}
$$

Taking summation over T iterations, we have:

$$
\frac{\gamma_0}{2\sqrt{T}}\sum_{t=1}^{T}\mathbb{E}\|\nabla L(\boldsymbol{w}_t)\|^2 \leq \mathbb{E}[L(\boldsymbol{w}_0)] - \mathbb{E}[L(\boldsymbol{w}_T)] + (\beta M + \frac{1}{2}\beta^3 \sigma^2 d)\gamma_0^2 \sum_{t=1}^{T}\frac{1}{t} + \frac{1}{2}\beta^2 \sigma^2 d \gamma_0 \sum_{t=1}^{T}\frac{1}{\sqrt{t}}. \quad (25)
$$

This gives:

$$
\begin{aligned}
\frac{1}{T}\sum_{t=1}^{T}\mathbb{E}\|\nabla L(\boldsymbol{w}_t)\|^2 \leq & \frac{2\left(\mathbb{E}[L(\boldsymbol{w}_0)] - \mathbb{E}[L(\boldsymbol{w}_T)]\right)}{\gamma_0\sqrt{T}} + (2\beta M + \beta^3 \sigma^2 d)\gamma_0 \frac{\log T}{\sqrt{T}} + 2\beta^2 \sigma^2 d && (26)\\
\leq & \frac{2\left(\mathbb{E}[L(\boldsymbol{w}_0)] - \mathbb{E}[L(\boldsymbol{w}^*)]\right)}{\gamma_0\sqrt{T}} + (2\beta M + \beta^3 \sigma^2 d)\gamma_0 \frac{\log T}{\sqrt{T}} + 2\beta^2 \sigma^2 d, && (27)
\end{aligned}
$$

where $\boldsymbol{w}^*$ is the optimal solution. □

B Proof of Theorem 2

Proof

$$
\begin{aligned}
L(\boldsymbol{w}_{t+1}) \leq & L(\boldsymbol{w}_t) + \nabla L(\boldsymbol{w}_t)^\top (\boldsymbol{w}_{t+1} - \boldsymbol{w}_t) + \frac{\beta}{2}\|\boldsymbol{w}_{t+1} - \boldsymbol{w}_t\|^2 && (28)\\
= & L(\boldsymbol{w}_t) - \gamma_t \nabla L(\boldsymbol{w}_t)^\top \left[\lambda \nabla L_{\mathcal{B}_1}(\boldsymbol{w}_{t+1/2}) + (1-\lambda)\nabla L_{\mathcal{B}_2}(\boldsymbol{w}_t)\right] \\
& + \frac{\gamma_t^2 \beta}{2}\|\lambda \nabla L_{\mathcal{B}_1}(\boldsymbol{w}_{t+1/2}) + (1-\lambda)\nabla L_{\mathcal{B}_2}(\boldsymbol{w}_t)\|^2. && (29)
\end{aligned}
$$

$$
\begin{aligned}
\mathbb{E}[L(\boldsymbol{w}_{t+1})] \leq & \mathbb{E}[L(\boldsymbol{w}_t)] - \frac{\gamma_t^2\beta}{2}\|\nabla L(\boldsymbol{w}_t)\|^2 + \gamma_t^2 \beta \left(\lambda^2 M + (1-\lambda)^2 M\right) + \gamma_t^2 \beta^3 \lambda^2 \sigma^2 d \\
& - (1-\beta\gamma_t)\gamma_t \|\nabla L(\boldsymbol{w}_t)\|^2 + (1-\beta\gamma_t)\gamma_t \left(\frac{1}{2}\|\nabla L(\boldsymbol{w}_t)\|^2 + \frac{\gamma_t}{2}\lambda^2\beta^2\sigma^2 d\right) && (30)\\
= & \mathbb{E}[L(\boldsymbol{w}_t)] - \frac{1}{2}\|\nabla L(\boldsymbol{w}_t)\|^2 + \gamma_t^2 \beta M \left(2\lambda^2 - 2\lambda + 1\right) + \frac{1}{2}(1+\beta\gamma_t)\gamma_t \lambda^2 \beta^2 \sigma^2 d && (31)\\
& && (32)
\end{aligned}
$$

Taking summation over T iterations, we have:

$$
\begin{aligned}
\frac{\gamma_0}{2\sqrt{T}} \sum_{t=1}^{T} \mathbb{E}\|\nabla L(\boldsymbol{w}_t)\|^2 \leq & \mathbb{E}[L(\boldsymbol{w}_0)] - \mathbb{E}[L(\boldsymbol{w}_T)] + \left(\beta M(2\lambda^2 - 2\lambda + 1) + \frac{1}{2}\beta^3\lambda^2\sigma^2 d\right)\gamma_0^2 \sum_{t=1}^{T}\frac{1}{t} \\
& + \frac{1}{2}\beta^2\lambda^2\sigma^2 d\gamma_0 \sum_{t=1}^{T}\frac{1}{\sqrt{t}}.
\end{aligned} \tag{33}
$$

This gives:

$$
\frac{1}{T}\sum_{t=1}^{T}\mathbb{E}\|\nabla L(\boldsymbol{w}_t)\|^2 \leq \frac{2\left(\mathbb{E}[L(\boldsymbol{w}_0)] - \mathbb{E}[L(\boldsymbol{w}^*)]\right)}{\gamma_0\sqrt{T}} + \left(2\beta M(2\lambda^2 - 2\lambda + 1) + \beta^3\lambda^2\sigma^2 d\right)\gamma_0 \frac{\log T}{\sqrt{T}} + 2\beta^2\lambda^2\sigma^2 d.
$$

□

C ViT training

To train the vision transformer model (Dosovitskiy et al., 2021), we adopt Adam Kingma & Ba (2015) as the base optimizer and train the models on CIFAR-10/100 datasets from scratch with Adam, SAM, RWP, and m-RWP. Specifically, we select the ViT-S model with input size 32×32, patch size 4, number of heads 8, and dropout rate 0.1. We train the models for 400 epochs with a batch size of 256, an initial learning rate of 0.0001, and a cosine learning rate schedule. For ARWP, we set $\sigma = 0.001$, and for m-ARWP, we set $\sigma = 0.002$ and $\alpha = 0.5$. For SAM, we perform a grid search for ρ over $[0.001, 0.002, 0.005, 0.01, 0.05, 0.1, 0.2, 0.5]$ and finally select $\rho = 0.05$ for optimal.